International Journal of Statistics and Applied Mathematics 2023; SP-8(3): 630-634

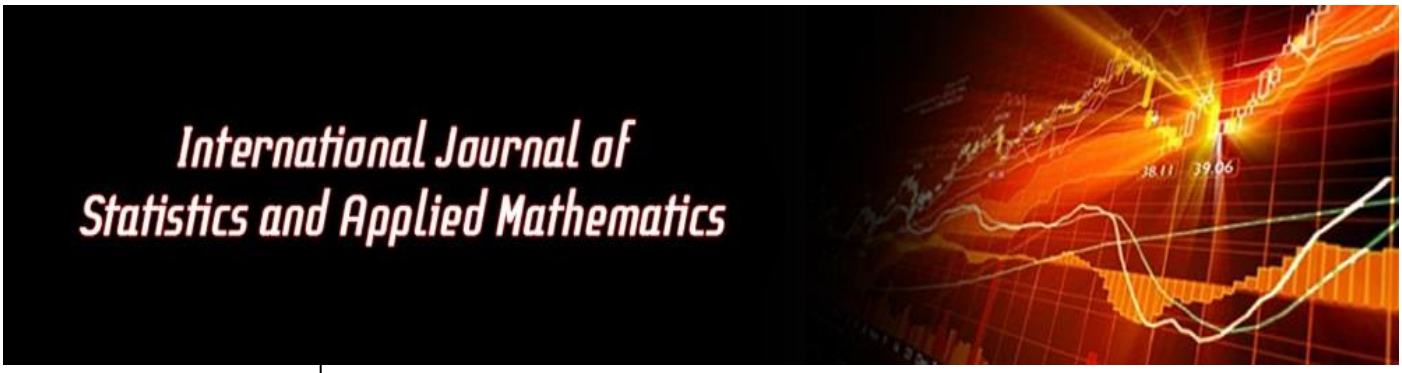

ISSN: 2456-1452
Maths 2023; SP-8(3): 630-634

https://www.mathsjournal.com
Received: xx-03-2023
Accepted: xx-04-2023

Somveer
Ph.D. Scholar, Dairy Engineering Division, ICAR-National Dairy Research Institute, Karnal, Haryana, India

F Magdaline Eljeeva Emerald
Principal Scientist, Dairy Engineering Division, ICAR-National Dairy Research Institute, Southern Regional Station, Bengaluru, Karnataka, India

Gursharn Singh Saini
Assistant Professor, Department of Dairy Engineering, College of Dairy Science and Technology, Guru Angad Dev Veterinary and Animal Sciences University, Ludhiana, Punjab, India

Manisha Kumari
Teaching Associate, Department of Dairy Engineering, College of Dairy Science and Technology, Rajasthan University of Veterinary and Animal Sciences, Bikaner, Rajasthan, India

Corresponding Author:
Somveer
Ph.D. Scholar, Dairy Engineering Division, ICAR-National Dairy Research Institute, Karnal, Haryana, India

Investigating structural changes of ZnO nanoparticles using powder X-ray diffraction over 6 months

Somveer, F Magdaline Eljeeva Emerald, Gursharn Singh Saini and Manisha Kumari

Abstract
In recent years, zinc oxide (ZnO) nanoparticles (NPs) have gained prominence as a remarkable metal oxide material, showcasing unique physical and chemical properties for heat transfer applications. The characterization of significant features relies on techniques such as powder X-ray diffraction (XRD) which unveils the structural properties and behavior of NPs. The influence of storage conditions on the XRD pattern of ZnO NPs was investigated in this study. Newly synthesized ZnO NPs were hermetically stored at room temperature for 6 months. The XRD pattern of ZnO NPs revealed distinct peaks at 2θ diffraction angles of 31.74, 34.40, 36.23, 47.53, 56.60, 62.87, 66.40, 67.97, and 69.10°, indicating their crystallization in a wurtzite hexagonal structure. Using the Debye Scherrer equation, the average crystallite size of the ZnO NPs was determined as 22.29 nm.

Keywords: Zinc oxide, powder X-ray diffractogram, wurtzite hexagonal structure, Debye-Scherrer equation

1. Introduction
Over the past few years, zinc oxide (ZnO) has emerged as a compelling metal oxide material due to its distinctive physical and chemical attributes. These include notable traits like exceptional chemical and mechanical stability, extensive radiation absorption capabilities, significant catalytic activity, electrochemical coupling coefficient, and inherent non-toxicity (Mohan and Renjanadevi, 2016) [9]. The prominent properties of nanoparticles (NPs) can be evaluated by using various characterization techniques like scanning electron microscope (SEM) and powder X-ray diffraction (XRD) etc. The structural properties and behavior of NPs are significantly reflected in their X-ray diffraction (XRD) pattern. XRD is used to determine the crystallographic structure, crystal structure, and size of NPs. ZnO has the potential to manifest as two-dimensional formations, including nano pellets and nanosheets/nanoplates (Kołodziejczak and Jesionowski, 2014) [5]. This research delves into the impact of storage conditions on the XRD pattern of ZnO NPs. Newly synthesized ZnO NPs were stored at ambient conditions for a duration of 6 months inside an airtight container. The analysis of alterations in the XRD pattern provided valuable insights into NPs stability, crystallinity, and potential phase changes. These discoveries enhance comprehension of the correlation between storage conditions and the XRD pattern of ZnO NPs, carrying implications for their practical utilization and characterization.

2. Materials and Methods
2.1 Storage of ZnO nanoparticles
The study aimed to examine the crystallographic structure, crystal structure, and size of ZnO NPs after a 6-months storage period. Freshly prepared ZnO NPs were prepared and stored in optimal conditions in an airtight plastic bottle at room temperature and pressure.

2.2 Sample preparation and testing
X-ray diffraction (XRD) is commonly used to measure the type, shape, and size of crystals. In this study, the ZnO NPs were analyzed using a powder X-ray diffractometer (Model: Rigaku SmartLab, Tokyo, Japan) within the 30-70° range of 2θ values (Fig. 1). The crystal analysis

was carried out using Cu-Kβ radiations with a wavelength of 0.139 nm, a goniometer speed of 0.02 s^{-1}, and applied voltage and current of 40 kV and 30 mA, respectively.

2.3 Powder X-ray diffraction parameters

The Scherrer constant and order of diffraction were taken as 0.9 and 1, respectively. The crystal size (D) was calculated from the 2θ values by using Debye-Scherrer's equation as given in equation 1 (Habib *et al.*, 2018) [1].

$$D = \frac{K\lambda}{\beta Cos\theta} \quad (1)$$

Where, D is crystal size (nm), K is Scherrer's constant, λ is wavelength of X-ray (nm), β is full width at half maximum (FWHM) of peaks and θ is the diffraction angle (radians) (He *et al.*, 2008). The crystallinity, micro strain (ε), dislocation density (δ) (Srinivasulu *et al.*, 2017; Murugan *et al.*, 2018) [14, 11], lattice parameters (hkl), bond lengths of Zn-O (l) (Sangeetha *et al.*, 2015) [13] values were determined from the equations 2, 3, 4, 5, and 6, respectively.

$$\text{Crystallinity} = \frac{\text{Area of maximum peaks}}{\text{Area of all peaks}} \times 100 \quad (2)$$

$$\varepsilon = \frac{\beta}{4\tan\theta} \quad (3)$$

$$\delta = \frac{1}{D^2} \quad (4)$$

$$\frac{1}{(d_{hkl})^2} = \frac{4}{3}\left[\frac{h^2+hk+k^2}{a^2}\right] + \frac{l^2}{c^2} \quad (5)$$

$$l = \sqrt{\left[\left(a^2/3\right) + \left(1/2 - u\right)^2 c^2\right]} \quad (6)$$

Where, ε is micro strain, β is FWHM of peaks (radians), θ is the diffraction angle (radians), δ is dislocation density (nm^{-2}), D is the crystallite size (nm), hkl are Miller indices, d_{hkl} are inter-planer spacing for the planes (hkl), 'a' and 'c' are lattice constants (nm/radians), 'l' is the length of bond parallel to c-axis (nm), 'u' is constant (nm/radians). Equation 7 was used to calculate the parameter 'u' (Basyooni *et al.*, 2017) [1]. The lattice constants i.e., a and c were calculated using equations 8 and 9, respectively.

$$u = \left(a^2/3c^2\right) + 0.25 \quad (7)$$

$$c = \frac{\lambda}{\sin\theta} \quad (8)$$

$$a = \frac{\lambda}{(3)^{1/3}\sin\theta} \quad (9)$$

Where, λ is wavelength of X-ray (nm) and θ is the diffraction angle (radians). The volume (V) of unit cell for the hexagonal system and interplanar space was computed by using equations 10 and 11, respectively.

$$V = \frac{\sqrt{3}}{2} a^2 c \quad (10)$$

$$d = \frac{n\lambda}{2\sin\theta} \quad (11)$$

Where, V is the volume of unit cell (nm^3) and n is order of diffraction (n=1). Equations 12 and 13 were used to calculate the porosity of particles.

$$\text{Porosity}\,(\%) = \left(1 - \frac{\rho_x}{\rho_T}\right) \times 100 \quad (12)$$

$$\rho_x = \frac{4M}{\sqrt{3} N_A a^2 c} \quad (13)$$

Where, N_A is Avogadro's number (6.02×10^{23}), M is molecular weight (kg/mol), ρ_x is density calculated from XRD data and ρ_T is the theoretical density (kg/m^3).

Fig 1: Powder X-Ray Diffractometer

The growth of (hkl) planes and crystalline orientation were computed in terms of texture coefficient $T_{c(hkl)}$ by using equation 14.

$$T_{c(hkl)} = \frac{\left(\frac{I_{(hkl)}}{I_{o(hkl)}}\right)}{\left[\frac{1}{n\sum\left(\frac{I_{(hkl)}}{I_{o(hkl)}}\right)}\right]} \quad (14)$$

Where, $I_{(hkl)}$ are the measured XRD intensities of planes (hkl) and $I_{0(hkl)}$ is standard XRD intensities of planes (hkl).

2.4 Data analysis

The data obtained from XRD testing of ZnO NPs was interpreted. Equation 15 was used to compute peak positions (2θ) values and FWHM values. The COD (R^2) value was maintained at approximately 1. The obtained characteristic spectral peaks were compared with the standard values taken from the International Centre for Diffraction Data (ICDD) card No. 00-036-1451 (Zelekew *et al.*, 2021) [15]. After analyzing the results, XRD planes graph was drawn and MS Excel was used to calculate all the parameters.

$$y = y_0 + \frac{A}{w\sqrt{\pi/2}} e^{-2\frac{(x-x_c)^2}{w^2}} \quad (15)$$

3. Results and Discussions

The XRD analysis was carried out within the range of 30 to 70° diffraction angles in order to examine various properties of biogenically synthesised ZnO NPs. These properties include crystal size, micro strain, inter-planar space, and crystallinity. During analyzing the XRD data, the monopolar distribution condition was taken (Fig.2). The Gauss Fit or NLFit was done as shown in figure 3, which resulted in 0.9949 COD (R^2) value and almost complete coverage of XRD graph (Fig. 4).

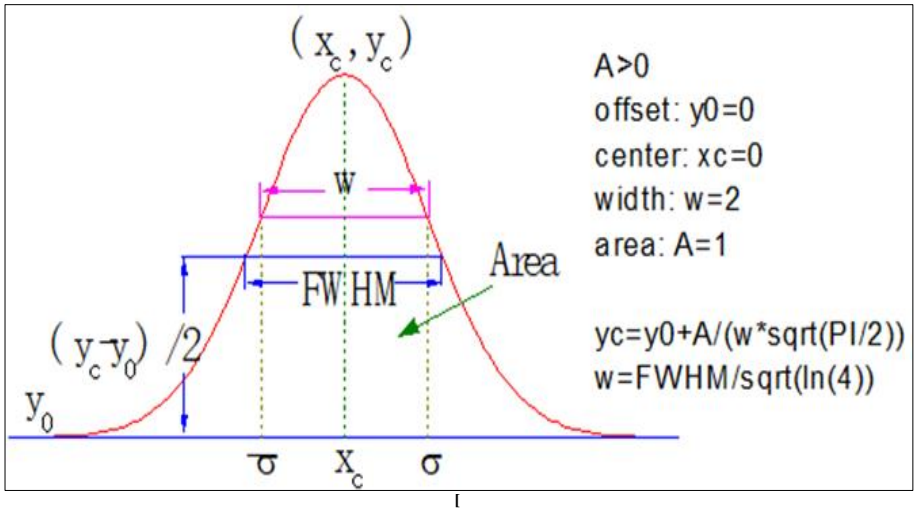

Fig 2: Monopolar Distribution Model

The analysis revealed specific spectral peaks at 31.74, 34.40, 36.23, 47.53, 56.60, 62.87, 66.40, 67.97, and 69.10°, which correspond to the various planes (100), (002), (101), (102), (110), (103), (200), (112), and (201) planes, respectively as shown in table 1 and figure 5. Similar results were obtained by researchers for freshly prepared samples of ZnO NPs (Ristic *et al.*, 2005; Madathil *et al.*, 2007) [12, 8]. The micro strain values exhibit a noticeable upward trend as the diffraction angles increase. The lowest micro strain value of 0.6750 was obtained at a diffraction angle of 30°, whereas the highest micro strain value of 1.40 was recorded at a diffraction angle of 69.10°. The XRD data enabled the calculation of the average dislocation density of ZnO NPs, which was determined to be 6.91×10^{-3} nm^{-2}. The purity of ZnO NPs was verified based on the absence of any significant peaks other than ZnO. The crystal size of ZnO NPs was determined to be 22.29 nm using Debye-Scherrer's equation (Eq. 1) The obtained findings were in good agreement with the results concluded by other researchers as the crystal size of fresh ZnO NPs was found to be in the range of 30-50 nm (Kumar *et al.*, 2015) [6], from 19 to 36 nm (Lahure *et al.*, 2015) [7], approximately 25 nm (Mohan and Renjanadevi, 2016) [9]. The inter-planer space and spectral peaks were in agreement with the standard values from ICDD card No. 00-036-1451. The degree of sharpness observed in the peaks reflects the crystalline nature of the samples, and the exclusive presence of the ICDD card No. 00-036-1451 peak suggested that the samples retained their original purity even following a storage duration of six months. The sharp peaks, as illustrated in figure 5, indicate the higher crystallinity (67.02%) and smaller size (22.29 nm) of the ZnO NPs. The lattice parameters from XRD analysis yielded values of 2.64 Å for a and b, and 3.79 Å for c. The values of a, b and C for fresh ZnO NPs were 3.25, 3.25 and 5.21 Å (Moussa *et al.*, 2022) [10]. The obtained results for ZnO NPs after 6 months study shown similarity with the findings of previous researchers (Mohan and Renjanadevi, 2016) [9]. The value of 'u' was determined to be 0.411, and the mean volume of the unit cell was calculated as 0.024 $Å^3$.

Table 1: Powder X-ray Diffraction Analysis of ZnO Nanoparticles

2θ (degree)	(hkl) planes	D (standard)	d (observed)	Micro strain (ε)	Texture coefficient (TC)	Dislocation density (δ) (10^{-3} nm^{-2})
31.744	100	2.814	2.818	0.422	0.999	1.697
34.405	002	2.603	2.607	0.463	0.999	1.703

36.236	101	2.476	2.480	0.502	0.999	1.775
47.550	102	1.911	1.914	0.769	1.000	2.126
56.601	110	1.625	1.627	0.967	1.000	2.084
62.878	103	1.477	1.479	1.173	1.000	2.230
66.401	200	1.407	1.409	1.198	1.000	1.953
67.972	112	1.378	1.379	1.380	1.000	2.398
69.100	201	1.358	1.360	1.405	1.000	2.350

The structure of ZnO NPs was determined to be wurtzite hexagonal in nature. The porosity and bulk density of ZnO NPs were determined to be 1.31% and 0.4923 g/cm^3, respectively. The TC_{hkl} values ranged from 0.999 to 1.000, indicating the orientation of crystals in the (100) and (201) planes. The average bond length was calculated as 1.559 Å and the crystallinity of ZnO crystals was found to be 67.02%.

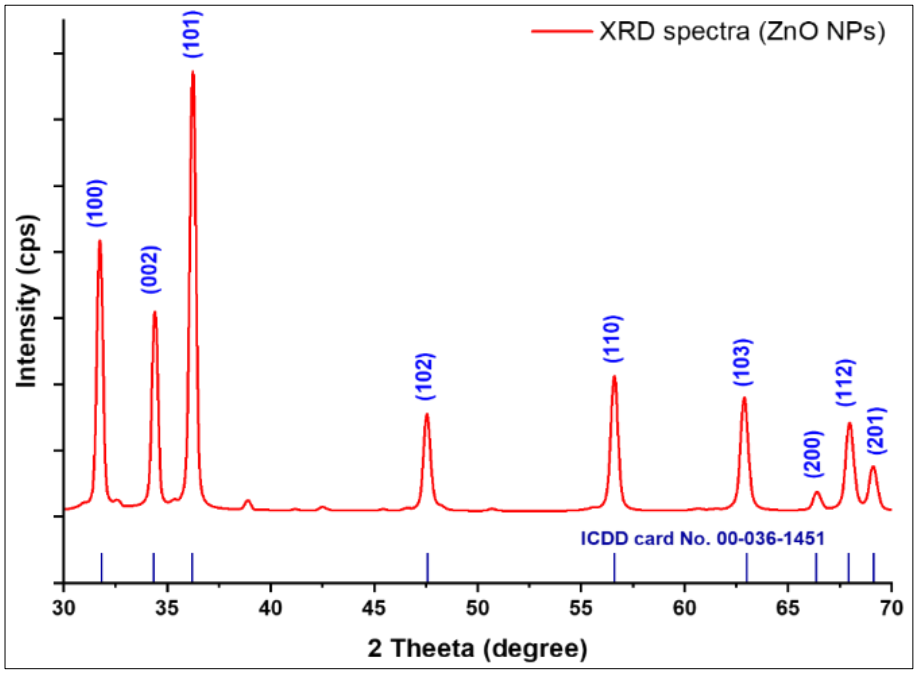

Fig 5: Powder X-ray Diffractogram of ZnO Nanoparticles after 6 Months Storage

4. Conclusion

The X-ray diffractograms of ZnO NPs exhibited distinct and strong peaks located at 2θ diffraction angles of 31.74, 34.40, 36.23, 47.53, 56.60, 62.87, 66.40, 67.97, and 69.10°. These patterns elucidated the crystallization of ZnO NPs in a wurtzite hexagonal structure. The application of the Debye Scherrer equation yielded an average crystallite size of 22.29 nm for the ZnO NPs. Notably, the observed inter-planar spacing (d spacing) between atoms closely aligned with the standard values of ICDD card no. 00-036-1451, affirming the exceptional purity of the ZnO NPs after 6 months storage duration. The obtained results were compared with the available literature and results showed good agreement with the previous results.

6. Acknowledgment

The authors express their gratitude for the assistance provided by the Department of Dairy Engineering at ICAR-National Dairy Research Institute, Karnal (Haryana), and for the facilities extended by CeNSE at the Indian Institute of Science, Bengaluru. These resources were funded by the Ministry of Education (MoE), Ministry of Electronics and Information Technology (MeitY), and Nano-mission of the Department of Science and Technology (DST), Government of India.

7. References

1. Basyooni MA, Shaban M, El Sayed AM. Enhanced gas sensing properties of spin-coated Na-doped ZnO nanostructured films. Scientific Reports. 2017;7(1):41716.
2. Habib IY, Kumara NTRN, Lim CM, Mahadi AH. Dynamic light scattering and zeta potential studies of ceria nanoparticles. Solid State Phenomena. 2018;278:112-120.
3. Habib IY, Tajuddin AA, Noor HA, Lim CM, Mahadi AH, Kumara NTRN. Enhanced Carbon monoxide-sensing properties of Chromium-doped ZnO nanostructures. Scientific Reports. 2019;9(1):9207.
4. He C, Sasaki T, Shimizu Y, Koshizaki N. Synthesis of ZnO nanoparticles using nanosecond pulsed laser ablation in aqueous media and their self-assembly towards spindle-like ZnO aggregates. Applied Surface Science. 2008;254(7):2196-2202.
5. Kołodziejczak-Radzimska A, Jesionowski T. Zinc oxide-from synthesis to application: a review. Materials. 2014;7(4):2833-2881.
6. Kumar M, Kumar S, Parveen Z, Kaur J, Sharma N, Bansod BS. Facial synthesis of nano sized ZnO by hydrothermal method. International Journal of Advanced Research in Electrical, Electronics and Instrumentation Engineering. 2015;4(5):4440-4444.
7. Lahure P, Salunke P, Soliwal R, Yadav A, Tripathi S, Koser AA. Plasma X-ray diffraction study of ZnO nanoparticles. International Journal of Scientific Research in Physics and Applied Sciences. 2015;3(1):32-33.

8. Madathil ANP, Vanaja KA, Jayaraj MK. Synthesis of ZnO nanoparticles by hydrothermal method. In Nanophotonic Materials IV. 2007 Sept;6639:47-55. SPIE.
9. Mohan AC, Renjanadevi BJPT. Preparation of zinc oxide nanoparticles and its characterization using scanning electron microscopy (SEM) and X-ray diffraction (XRD). Procedia Technology. 2016;24:761-766.
10. Moussa N, Ebrahim FM, Adly K, Hassaan MY. XRD, structural, optical, electrical and magnetic properties of ZnO nanoparticles incorporated with Cr as a promising material for different applications. Research Square. 2022;1(1):1-26.
11. Murugan R, Kashinath L, Subash R, Sakthivel P, Byrappa K, Rajendran S, *et al*. Pure and alkaline metal ion (Mg, Ca, Sr, Ba) doped cerium oxide nanostructures for photo degradation of methylene blue. Materials Research Bulletin. 2018;97:319-325.
12. Ristić M, Musić S, Ivanda M, Popović S. Sol-gel synthesis and characterization of nanocrystalline ZnO powders. Journal of Alloys and Compounds. 2005;397(1-2):L1-L4.
13. Sangeetha R, Muthukumaran S, Ashokkumar M. Structural, optical, dielectric and antibacterial studies of Mn doped Zn0.96Cu0.04O nanoparticles. Spectrochimica Acta Part A: Molecular and Biomolecular Spectroscopy. 2015;144:1-7.
14. Srinivasulu T, Saritha K, Reddy KR. Synthesis and characterization of Fe-doped ZnO thin films deposited by chemical spray pyrolysis. Modern Electronic Materials. 2017;3(2):76-85.
15. Zelekew OA, Aragaw SG, Sabir FK, Andoshe DM, Duma AD, Kuo DH, *et al*. Green synthesis of Co-doped ZnO via the accumulation of cobalt ion onto *Eichhornia crassipes* plant tissue and the photocatalytic degradation efficiency under visible light. Materials Research Express. 2021;8(2):025010.